

This article was downloaded by:

On: 26 January 2011

Access details: *Access Details: Free Access*

Publisher *Taylor & Francis*

Informa Ltd Registered in England and Wales Registered Number: 1072954 Registered office: Mortimer House, 37-41 Mortimer Street, London W1T 3JH, UK



## Liquid Crystals

Publication details, including instructions for authors and subscription information:

<http://www.informaworld.com/smpp/title~content=t713926090>

### Heat capacity peaks observed at the blue phase transitions in compounds of different purities

P. Taborek<sup>ab</sup>; J. W. Goodby<sup>ac</sup>; P. E. Cladis<sup>a</sup>

<sup>a</sup> AT&T Bell Laboratories, Murray Hill, New Jersey, U. S. A. <sup>b</sup> Texas Instruments Central Research Laboratories, Dallas, Texas, U. S. A. <sup>c</sup> School of Chemistry, The University of Hull, Hull, England

**To cite this Article** Taborek, P. , Goodby, J. W. and Cladis, P. E.(1989) 'Heat capacity peaks observed at the blue phase transitions in compounds of different purities', *Liquid Crystals*, 4: 1, 21 – 37

**To link to this Article:** DOI: 10.1080/02678298908028956

**URL:** <http://dx.doi.org/10.1080/02678298908028956>

PLEASE SCROLL DOWN FOR ARTICLE

Full terms and conditions of use: <http://www.informaworld.com/terms-and-conditions-of-access.pdf>

This article may be used for research, teaching and private study purposes. Any substantial or systematic reproduction, re-distribution, re-selling, loan or sub-licensing, systematic supply or distribution in any form to anyone is expressly forbidden.

The publisher does not give any warranty express or implied or make any representation that the contents will be complete or accurate or up to date. The accuracy of any instructions, formulae and drug doses should be independently verified with primary sources. The publisher shall not be liable for any loss, actions, claims, proceedings, demand or costs or damages whatsoever or howsoever caused arising directly or indirectly in connection with or arising out of the use of this material.

## Heat capacity peaks observed at the blue phase transitions in compounds of different purities

by P. TABOREK†, J. W. GOODBY‡ and P. E. CLADIS

AT&T Bell Laboratories, 600 Mountain Avenue, Murray Hill, New Jersey 07974, U.S.A.

(Received 23 May 1988; accepted 23 July 1988)

Latent heat measurements, determined by high resolution and slow temperature scanning calorimetry ( $10^{-30}$ C/min), in three compounds of differing purity—where any enantiomer of opposite handedness to that of the predominant enantiomer is included in the impurity count—suggest a correlation between blue phase stability and material purity when chiral excess is included in estimates of impurity, the data suggest that materials with less than  $\sim 1.3$  per cent impurities present will not exhibit blue phases even though their pitch is small enough to support blue phases. One class of compounds is discussed where this condition may indeed apply. Furthermore, the magnitude of the total latent heat of blue phase transitions was observed to be sensitive to scan rates: a significantly smaller latent heat was measured at the slowest scan rates compared to faster scan rates and the magnitude of the difference was largest for the isomerically purest compound.

### 1. Introduction

When a short pitched ( $\lesssim 4000$  Å) cholesteric is heated to within half a degree or so of the isotropic phase, it frequently undergoes transitions to one to three intermediate states called blue phases [1-3] referred to as BPI, BPII and BPIII. The structure of BPI and BPII is a cubic lattice of defects with a lattice constant comparable to the pitch. No evidence for a lattice structure has been found for BPIII.

Although blue phases are homogeneous phases on scales larger than the pitch, on smaller scales they are believed to be inhomogeneous. They occur within a range of temperatures comparable to the usual two phase region observed at the cholesteric-isotropic transition or nematic-isotropic transition [4]. The director configuration that is locally an energy minimum, called 'double twist' [5] cannot fill space uniformly, and an array of defects filled with the isotropic phase in their core regions, is required to make a large scale homogeneous phase. If the 'double twist'-isotropic interfacial energy is sufficiently low, this defect array state may be the global free energy minimum of the system. At still lower temperatures, it costs too much energy to create the defect array so, the material reorganizes itself into the usual singly twisted structure. Thus, blue phases are examples of frustrated structures in equilibrium [3].

An outstanding fundamental question raised by blue phases is: can really pure materials form blue phases? In this paper, we probe the role of impurities, including opposite handed enantiomers as an impurity, in stabilizing these interesting phases

† Present address: Texas Instruments Central Research Laboratories, Dallas, Texas 75265, U.S.A.

‡ Present address: School of Chemistry, The University of Hull, Hull HU6 7RX, England.

exhibited by chiral molecules, using calorimetry and liquid chromatography. Our main results may be summarized as follows:

- (1) High resolution, slow scanning ( $10^{-3}\text{C}/\text{min}$ ) calorimetry found little difference in the width of latent heat peaks at blue phase transitions between a compound determined by high performance liquid chromatography to be at least 99.5 per cent pure and one that was at most only 90 per cent pure. Although 99.5 per cent isomerically pure, one chiral compound was determined to have an enantiomeric excess (defined as the difference in percent of the two chiral species) of 80 per cent: 10 per cent of the material was structured with the opposite hand of 90 per cent of the material. Because its latent heat peaks were as broad as materials that are only 90 per cent pure, we are led to conclude that although isomerically indistinguishable, 10 per cent of the opposite hand acts as an impurity in blue phase formation.
- (2) The data show a trend to shorter temperature ranges for blue phases with increasing sample purity suggesting that chiral materials with less than 1.3 per cent impurity, including the opposite handed enantiomer as an impurity, may not exhibit blue phases. Impurities can form the cores of defect arrays and so energetically favor the structure of blue phases. We discuss one material that may be too pure to exhibit blue phases even though its pitch is short enough.
- (3) Finally, we found that latent heats obtained at scanning rates of  $10^{-3}\text{C}/\text{min}$  were smaller than obtained at  $0.5\text{C}/\text{min}$ . The dependence on scan rate appeared correlated to isomeric sample purity: the purest compound exhibited the largest difference. This result suggests that purer materials take longer to reach equilibrium at blue phase transitions than less pure materials, providing another indication of the role impurities may play in the dynamics of frustrated systems such as blue phases.

## 2. Experiment and observations

The materials studied were cholesteryl nonanoate (CN), cholesteryl myristate (CM) and S-(+)-4-(2'-methylbutyl)phenyl 4-*n*-octylbiphenyl-4'-carboxylate (8SI\*, also known as CE8 now manufactured by BDH Chemicals). The cholesteryl derivatives were purchased from van Schuppen (VS) and Eastman Kodak (EK). 8SI\* was synthesized as described previously [6, 7]. The three blue phases of CN and the two of 8SI\* are easily observed by optical microscopy. However, the two blue phases of CM are difficult to observe in this way because the pitch is in the short range of optical wave lengths.

### 2.1. Characterizing sample purity using liquid chromatography

The purities of the individual compounds were investigated by high performance liquid chromatography using a Beckman 334 solvent delivery system in conjunction with a 421 controller and 164 variable wavelength UV/visible detector. The chromatographic separations for CM and CN were carried out over octadecylsiloxane (Dupont Zorbax ODS,  $5\mu\text{m}$  pore size,  $25 \times 0.46\text{cm}$ ) using hexane (Aldrich) as the eluant. The absorption of the eluting fractions was monitored at four different wavelengths:  $\lambda = 220, 225, 230, \text{ and } 235\text{ nm}$ . For 8SI\*, the chromatographic separation was also carried out over octadecylsiloxane (Zorbax ODS  $5\mu\text{m}$  pore size,  $25 \times 0.46\text{cm}$ ) using acetonitrile as the eluant. The absorption of the eluting fractions was monitored at  $255\text{ nm}$ .

The traces from the chromatography for the three compounds are shown in figures 1, 2 and 3. The vertical axis is the relative absorption of the eluting fractions at a given wavelength,  $\lambda$  (nm). The horizontal axis is the retention time on the column in minutes. The precise purities of CM and CN cannot be determined directly by high performance liquid chromatography because the relative absorptions of the cholesteryl esters and the impurities that they contain are not known at the wavelengths investigated. To determine these values accurately, it would be necessary to separate out all of the components in each sample and determine their relative absorptions with respect to wavelength, as a function of concentration in standard solutions. This would involve shaving complex and broad peaks in a number of the samples, which in turn could lead to further inaccuracies.

However, it is possible to obtain an estimate of the material purity by making use of the following information. First, cholesteryl esters are essentially aliphatic systems and therefore strongly absorb in the region of 200–220 nm—the U.V. cut-off for the hexane eluant being 195 nm. Second, the impurity(ies) showed a relatively constant absorption over the wavelength range investigated. And, third, at wavelengths over 250 nm, very little U.V. radiation was absorbed indicating the near absence of aromatic impurities.

Thus, a lower limit of the impurity concentration is obtained at the shortest wavelength tested. This wavelength was selected to be 220 nm. At shorter wavelengths, the eluant starts to contribute to the absorption and the relative absorptions of the impurities tend to decrease. The table summarizes the purity of the two stocks of cholesteryl esters at the various wavelengths tested.

Purity of cholesterol nonanoate and cholesterol myristate in per cent as a function of wavelength deduced from data shown in figures 1 and 2.

Wavelength, $\lambda$ nm	Ch. nonanoate		Ch. myristate	
	VS	EK	VS	EK
	(per cent)			
235	70.9	55	92	47.7
230	79.3	63.4	93.6	48.3
225	82.9	74	96.2	48.6
220	89.6	93.8	97	70.8

For an example of pure compounds exhibiting blue phases we chose 8SI\*. Its trace is shown in figure 3. From the absence of secondary peaks, it was judged to be at least 99.5 per cent chemically pure, the approximate limit of resolution of the instrument.

Materials like 8SI\*, have the advantage that their structure is sufficiently simple that optical and chemical purities can be well-defined and they are more easily purified than cholesteryl compounds. The cholesteryl moiety is not synthesized from starting materials with a known purity but derived from naturally occurring substances that can sometimes be very complex. It contains many optically active sites so that an enantiomeric excess cannot be easily characterized.

We estimate the enantiomeric excess in 8SI\* to be about 80 per cent. This estimate is arrived at by determining the optical purity of the precursor S-4-(2'-methylbutyl)-phenol used in the synthesis of 8SI\*. This phenol was reacted with L-mandelic acid to give a mixture of diastereoisomers. This mixture was separated by chromatography and the relative peak areas of the diastereoisomers were used to calculate the optical purity of the starting chiral alcohol.

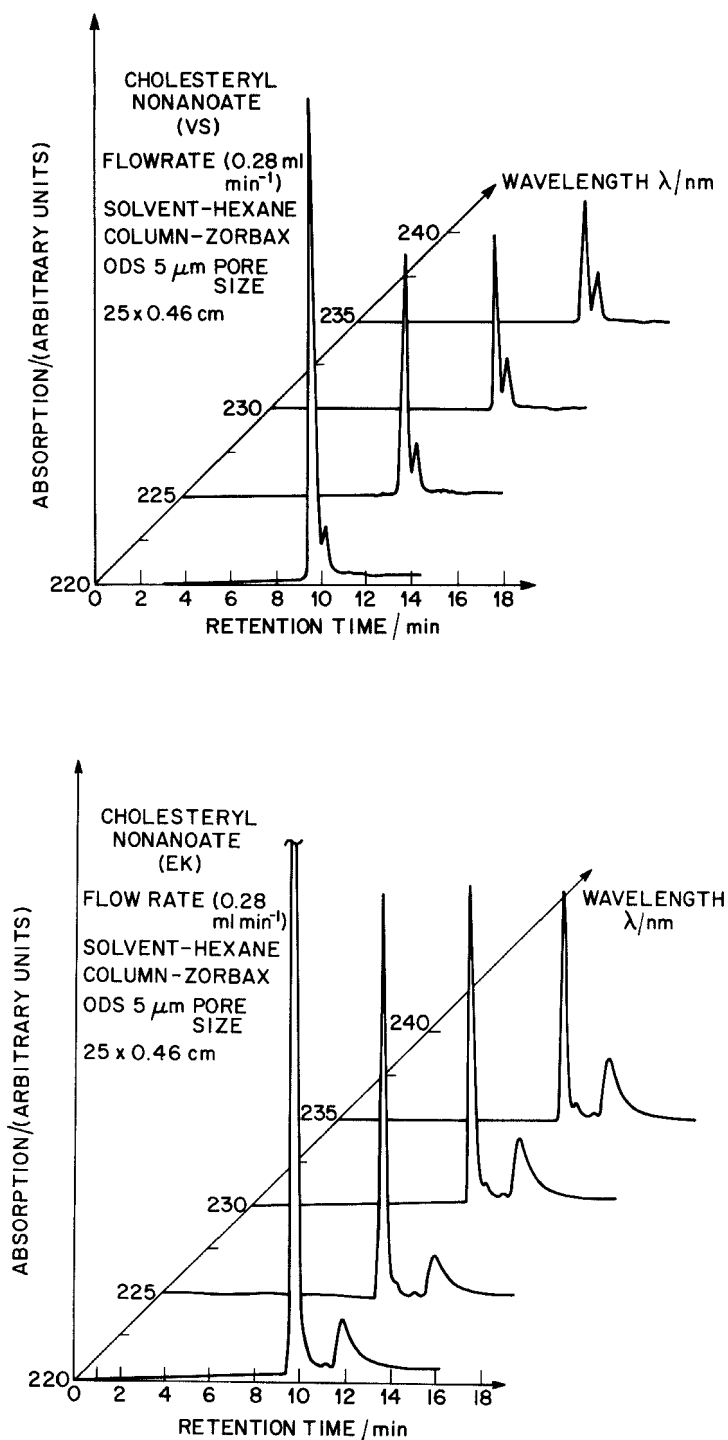


Figure 1. High resolution chromatographic data for the two stocks of cholesterol nonanoate (a) van Schuppen and (b) Eastman Kodak at various wavelengths. The vertical axis is the absorption of the eluting fraction at a given wavelength,  $\lambda$  (nm). The horizontal axis is the retention time on the column in minutes.

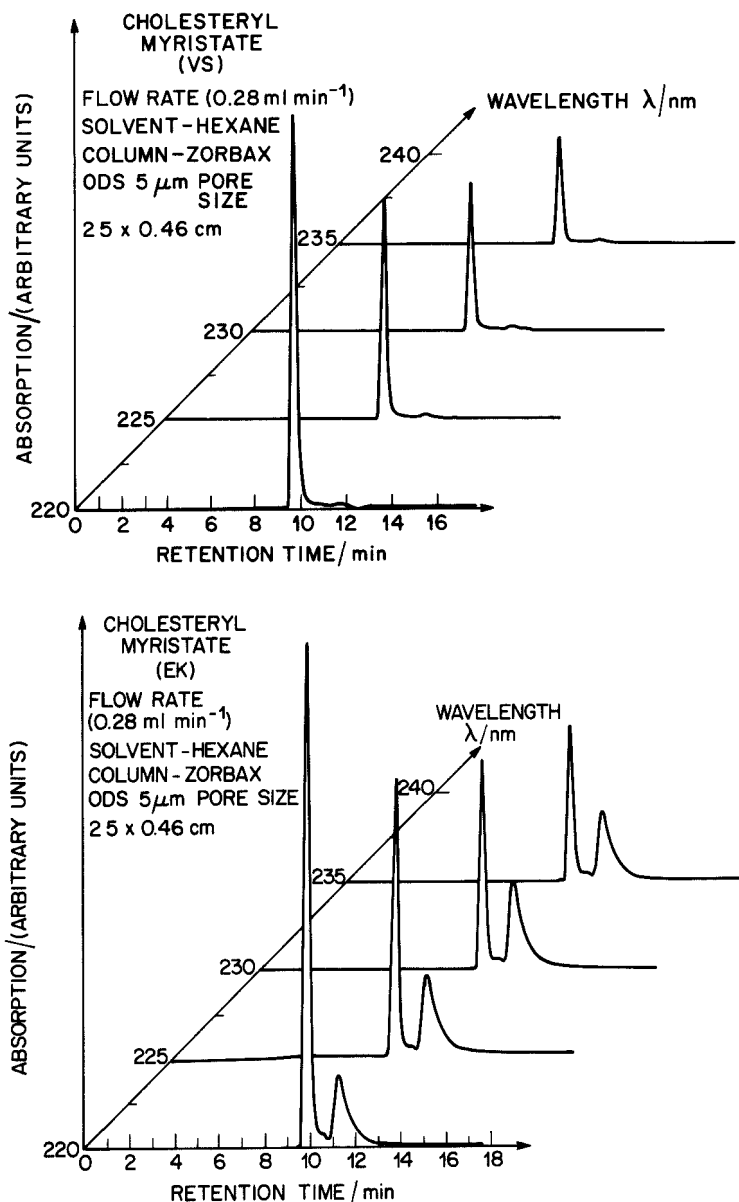


Figure 2. High resolution chromatographic data for the two stocks of cholesterol myristate (a) van Schuppen and (b) Eastman Kodak at various wavelengths (nm). Axes as in figure 1.

### 2.2. Differential scanning calorimeter observations

We used a Perkin-Elmer D.S.C. 4 differential scanning calorimeter (D.S.C.) in conjunction with a TADS data analysis station. This instrument measures the different amounts of heat required to maintain two sample chambers at the same temperature. Each compartment is loaded with an aluminum sample pan and lid. Liquid crystal material is in one and air in the other. The lid is crimped to firmly fix it to the pan and to contain the sample. Movement of the lid or movement of the sample owing to flow patterns created at a transition, can lead to spurious peaks. The

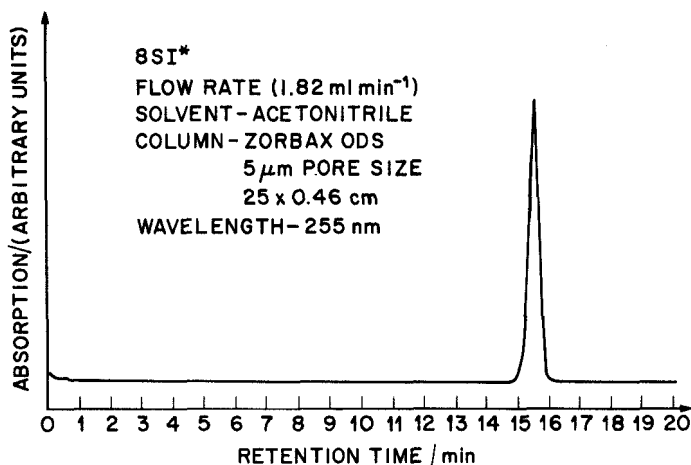


Figure 3. High resolution chromatography for 8SI\* monitored at 255 nm. Axes as in figures 1 and 2.

weight of the empty sample containers and lid is about 20 mg. Sample weights are typically 7–9 mg. Using two empty pans, a base line is measured and subtracted from the measurements.

As a check on the instrument, an indium standard (6.708 mg) was run at 0.5°C/min, the slowest speed of the instrument. The measured latent heat, 6.79 cal/g, compares well with 6.80 cal/g usually obtained for indium. The onset temperature 156.56°C also agrees well with the known melting point of indium (156.60°C). The half-width ( $\Delta T_{1/2}$ ) was found to be 0.14°C on heating and 0.04°C on cooling because the freezing transition super-cooled.

Figure 4 shows the trace observed for cholesteryl nonanoate (CN) while scanning at 0.5°C/min through the cholesteric to isotropic transition. The VS stock exhibits the narrower cholesteric to isotropic peak and a  $\Delta T_{1/2} = 0.28^\circ\text{C}$ . As the compound degrades, these traces become richer in structure and broader in temperature range (i.e. resemble the trace obtained for the EK stock). The total magnitude of the latent heat at this transition is 0.2 cal/g. This agrees well with the value found by Stegemeyer and Bergman [8]; 530 J/mole = 0.25 cal/g, taking the molecular weight of CN to be 526.89.

Similar data, found for CM, is shown in figure 5 (a) and (b). Here the EK stock shows a broad flat hump expected for a two phase region whereas the VS stock shows a sharper peak,  $\Delta T_{1/2} = 0.17^\circ\text{C}$ , and a substantially higher transition temperature. The latent heat is measured to be 0.25 cal/g or about the same as CN and one half the value found in [8] for CM, (1100 J/mole = 0.47 cal/g taking the molecular weight of CM to be 597.0). As will be discussed later, we believe that this discrepancy may be significant and related to scanning rates and impurity content of the material.

Figure 6 shows a typical plot of the D.S.C. trace on both heating and cooling of 8SI\*. A single well-defined peak with  $\Delta T_{1/2} = 0.25^\circ\text{C}$  is observed. The total heat of transition here is 0.4 cal/g. No structure is evident in these D.S.C. measurements of the smaller blue phase transitions.

Simultaneous with the D.S.C. measurements, microscopic observations were made on an independent sample of 8SI\* with a Mettler oven set to scan at the same

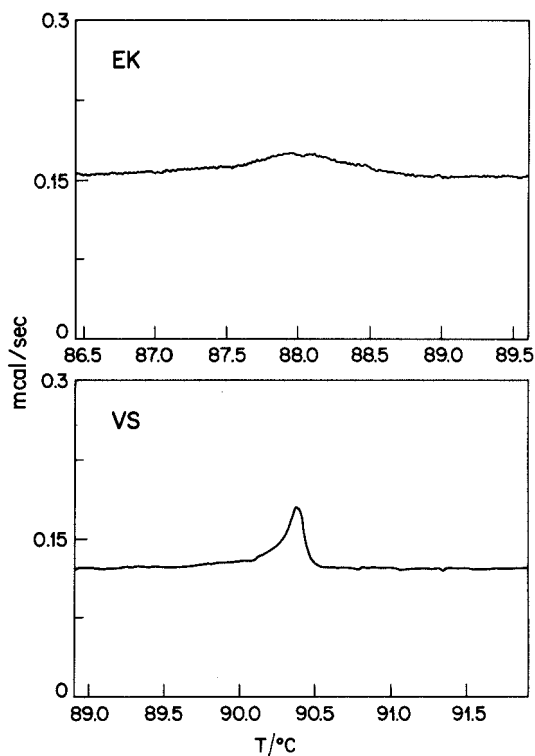


Figure 4. D.S.C. traces at  $0.5^{\circ}\text{C}/\text{min}$  for 9.50 mg cholesteryl nonanoate obtained from Eastman Kodak (top) and 7.57 mg obtained from van Schuppen (bottom). Although the EK stock shows a considerably broader peak owing to the larger fraction of impurity, the area under both peaks corresponds to a latent heat of  $0.2\text{ cal/g}$ . The onset temperatures are  $87.65^{\circ}\text{C}$  for the EK stock and  $90.22^{\circ}\text{C}$  for the VS stock.

temperature rate as the calorimeter. In this way the calculated onset temperature was observed to correspond to better than  $0.1^{\circ}\text{C}$  to the appearance of blue phases both in the heating and cooling cycle. On figure 6, arrows, marking the temperature range of the blue phases determined by observations in the optical microscope, show that the blue phase transitions are not resolved by this instrument.

Published results on measuring blue phase transition heats using D.S.C. are mixed. Several authors [9, 10] are not able to observe the transitions between cholesteric-BPI, BPI-BPII and BPII-BPIII transitions. Stegemeyer and Bergmann [8] and Armitage and Price [10] observed small latent heat peaks at the cholesteric-BPI and BPI-BPII transitions and an enormous latent heat at the blue fog to isotropic transition using a D.S.C. 2 and scan rates as slow as  $0.6^{\circ}\text{C}/\text{min}$ . Armitage points out in his case that these peaks are not always observed and they have never been observed on cooling, even when the blue phase supercools into the cholesteric phase. Stegemeyer [8], using gold pans and scanning rates comparable to Armitage and ours, obtained clear peaks at these transitions.

Most recently, latent heat peaks have been observed at blue phase transitions using high resolution calorimetry [12]. Rather than modifying our D.S.C. measurements, we decided a better strategy was to use this technique since scanning rates were three orders of magnitude slower and temperature differences could be measured with a resolution two orders of magnitude better than in a D.S.C. 4.



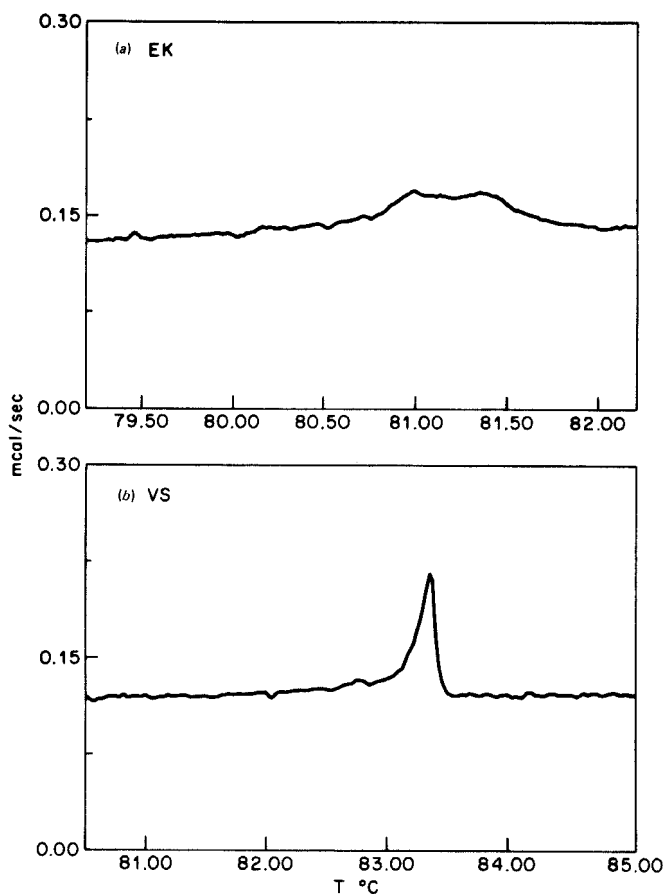


Figure 5. D.S.C. trace of (top) EK and (bottom) VS stock of CM taken at a scanning rate of  $0.5^{\circ}\text{C}/\text{min}$ . The 8.97 mg of the EK stock shows a broad small flat topped hump with an integrated heat capacity of  $0.2\text{ cal}/\text{gram}$ . The onset temperature is  $80.8^{\circ}\text{C}$ . 7.52 mg of VS stock shows a sharp peak with an integrated heat capacity of  $0.25\text{ cal}/\text{g}$ . Its onset temperature is  $83.2^{\circ}\text{C}$ .

### 2.3. High resolution slow scanning calorimetry

This calorimeter uses a single sample cell with a volume of  $0.9\text{ cm}^3$  [3]. The cell is made of gold plated brass and is sealed with a vacuum tight indium O-ring. A heater wire and thermistor are bonded to the outside of the cell. The cell is filled with a molten sample in an argon atmosphere glove box. The internal thermal time constant of the loaded cell is reduced to approximately 30 s by including a spiral of high conductivity gold foil. The sample is suspended by fine wires in a copper vacuum can that serves as a thermal shield. The shield is isolated from the environment by a stainless steel vacuum can.

The thermistors used to monitor the temperature of the can and the shield, have a sensitivity of  $\sim 1000\text{ ohms}/^{\circ}\text{C}$ . The thermistors were incorporated as one arm of a Wheatstone bridge and the temperature was deduced by measuring the off-balance signal with a lock-in amplifier. Using this technique, we could measure temperature changes of  $10^{-4}\text{ }^{\circ}\text{C}$ . The absolute accuracy of the temperature readings is about  $0.7^{\circ}\text{C}$ , so no meaningful conclusion can be drawn in the discrepancies in the absolute

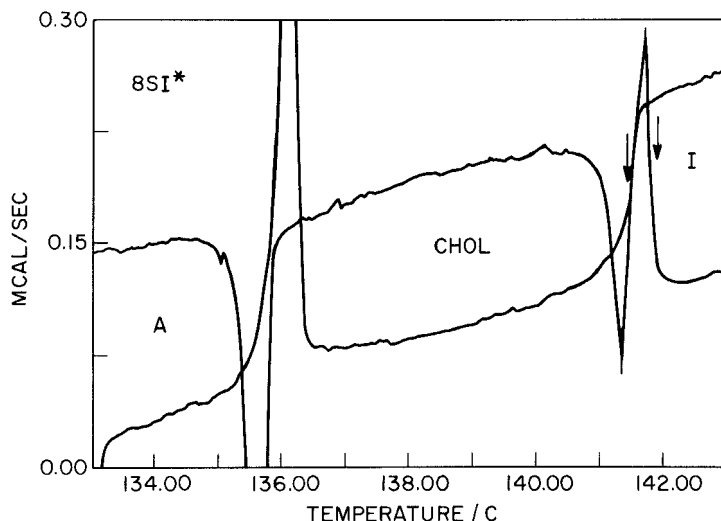


Figure 6. D.S.C. 4 trace of 9.19 mg of 8SI\*. Although the maximum in heating differs from the minimum in cooling by  $\sim 0.4^\circ\text{C}$ , the calculated onset temperature is identical in both cases:  $T_{\text{onset}} = 141.30^\circ\text{C}$  on heating and  $141.31^\circ\text{C}$  on cooling. On heating, the entire blue phase range occurs within the temperature range spanned by the heat of transition peak,  $141.38^\circ\text{C}$ – $142^\circ\text{C}$ . The cholesteric–isotropic heat of transition is  $0.4\text{ cal/g}$ . The off-scale peak is the transition to the smectic A phase. On cooling, a blue phase nucleated at  $142.2^\circ\text{C}$ . The arrows on the heating curve show the onset and end of the blue phase range observed by optical microscopy. Two blue phase transitions are clearly observed in the optical microscope.

transition temperature between this method and the D.S.C. that uses platinum thermometers calibrated against the melting transition of indium.

The heat capacity of the sample was determined by operating the calorimeter in a standard adiabatic mode in which stray heat leaks are minimized by servo-locking the shield temperature to the sample temperature and measuring the temperature rise of the sample due to a known heat input. For high resolution studies, it is more convenient to operate the calorimeter in either an increasing or decreasing temperature drift mode in which the shield temperature is ramped at a constant rate. The temperature is ramped by appropriately adjusting the set point of a PID controller using a six decade resistor with an IEEE interface.

After an initial transient, the response of the sample temperature is governed by:

$$C\dot{T} = \dot{Q}$$

where  $C$  is the sample heat capacity,  $\dot{Q}$  is the heat flux into the sample due to radiative heat transfer from the shield and  $\dot{T}$  is the rate of change of the sample temperature. Over the narrow range of temperatures considered here,  $\dot{Q}$  is proportional to the fourth power of the difference between the sample temperature,  $T$ , and the shield temperature,  $T_s$ . The proportionality factor can be determined by measuring the sample heat capacity at one temperature using the adiabatic method. The heat capacity at any other temperature can be determined by measurements of  $\dot{T}$  and  $\dot{Q} \propto T^4 - T_s^4$ . Typical drift rates of the shield temperature were  $\sim 10^{-3}^\circ\text{C}/\text{min}$  or about three orders of magnitude slower than possible with the standard Perkin-Elmer D.S.C.

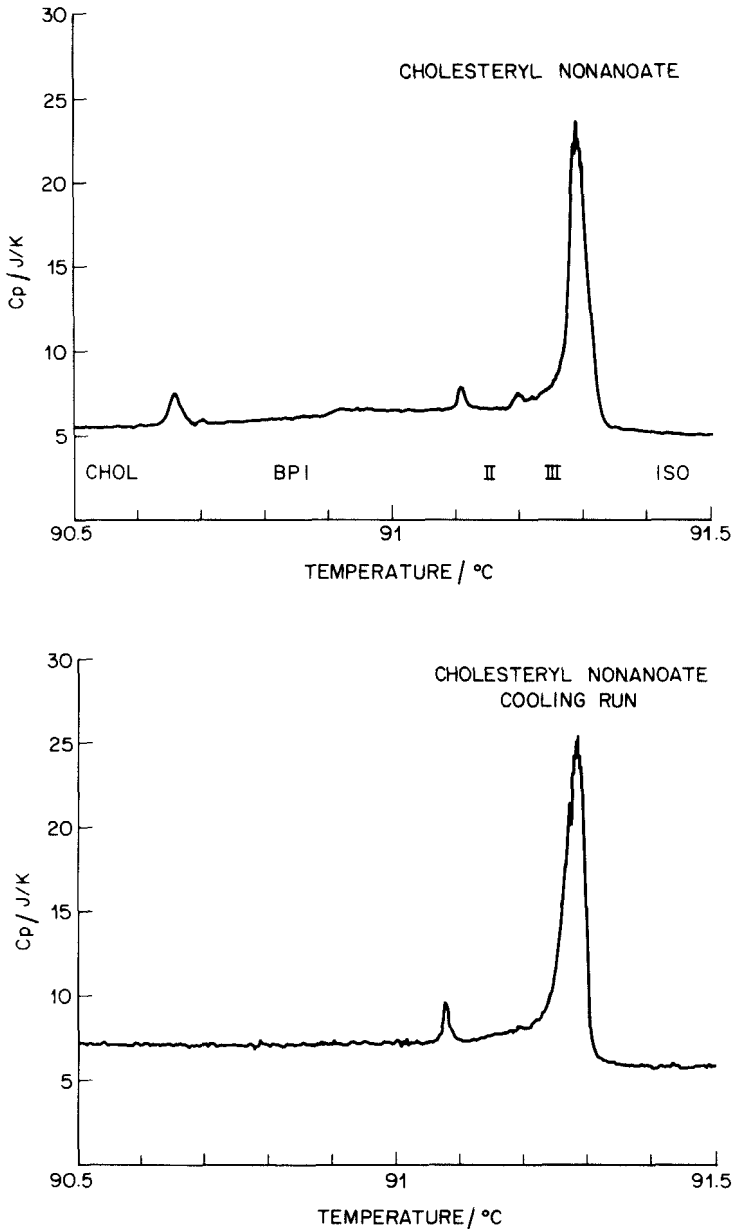


Figure 7. High resolution, slow scanning rate calorimetry of the VS stock of CN. (a) shows the heating run and (b) the cooling run. The largest peak is not resolution limited. Note that the temperature scale is only 1 $^{\circ}\text{C}$  wide. Sample mass is 1.89 g.

Figure 7(a) shows traces of the total heat capacity (sample plus container) observed for the VS stock of CN on heating. The peaks in the heat capacity are the signatures of first order phase transitions in the sample. Under ideal conditions of perfect sample purity and thermal homogeneity, these peaks would be delta functions. The latent heats of the phase transitions can be determined by measuring the area under the peaks. The largest peak is observed at 91.29 $^{\circ}\text{C}$  with a latent heat of

0.092 cal/g. This is the transition from BPIII to the isotropic phase. Its half-width, 0.03°C, is several times the instrumental resolution of the slow scanning apparatus, ~1 mK, and below the resolution of our D.S.C. The smaller peaks have half-widths comparable to the instrumental resolution, ~10 mK. The smallest peak with a latent heat of 0.0017 cal/g is observed at the BPII–BPIII transition, 91.20°C. Similar data for BPI–BPII and cholesteric–BPI are 91.11°C and 0.0022 cal/g and 90.66°C and 0.0054 cal/g.

The total latent heat for the transition from cholesteric to isotropic is 0.1813 cal/g and is comparable to the 0.21 cal/g measured by D.S.C. in this study and in [8]. In this compound, the blue phases span a temperature range of 0.63°C, slightly larger range than the 0.45°C range observed by Stegemeyer and Bergmann [8]. The magnitudes of the heats of transition of the blue phases are below the resolution of our D.S.C. apparatus. For comparison, values found by [8] for these transitions, are 0.0077 cal/g for cholesteric–BPI at 91°C and ~0.0077 cal/g at 91.3°C for BPI–BPII.

The cooling data is shown in figure 7(b). The BPII–BPI transition is clearly observed with a slight supercooling. It is somewhat sharper but with a similar magnitude for the total heat capacity as its counterpart observed in the heating cycle. The BPI–cholesteric transition is not observed because this transition super-cooled outside the temperature range shown. The BPIII–BPII peak is drowned in the slightly enlarged width of the BPIII–isotropic peak.

Figure 8 shows heat capacity data on heating for the VS stock of CM. The BPII–isotropic transition occurs at 84.11°C with a latent heat of 0.0018 cal/g; the BPI–BPII peak is at 84.05°C with 0.0013 cal/g and cholesteric–BPI at 83.95°C with 0.0798 cal/g. The combined latent heat of all these transitions, 0.0829 cal/g, is smaller by more than half the value found (0.25 cal/g) in the D.S.C. runs of this study and a quarter of the value found in [8]. It is curious to note that our measurements find

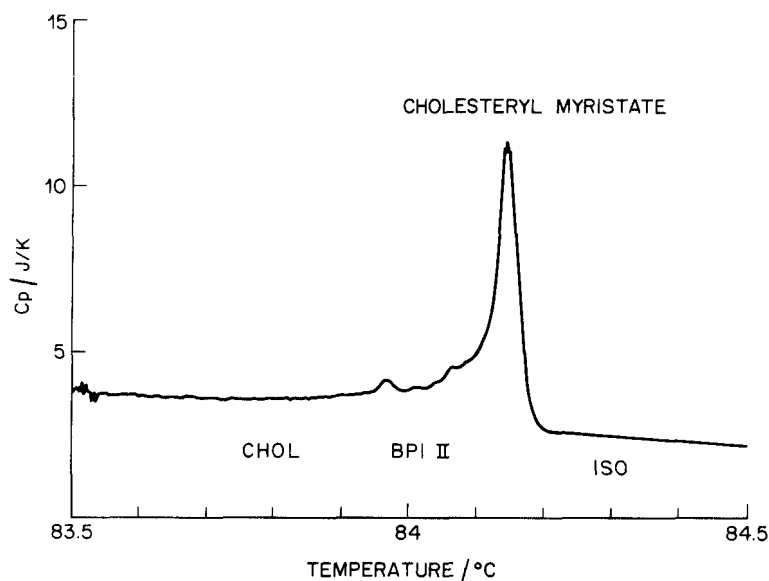


Figure 8. Heat capacity of CM taken under the same conditions as CN in figure 7. Sample mass is 0.98 g.

the total latent heat of CM to be about a half of CN whereas [8] finds the total latent heat of CM to be twice that of CN. For comparison, the magnitudes found by [8] for the cholesteric–BPI transition is 0.0136 cal/g at 84.0°C and ~0.0136 cal/g at 84.4°C.

Again, we note that the largest peak is broader than the instrumental resolution. In this case, the total temperature range of the blue phase transitions is only 0.16°C correlating with the higher purity of this sample compared to CN.

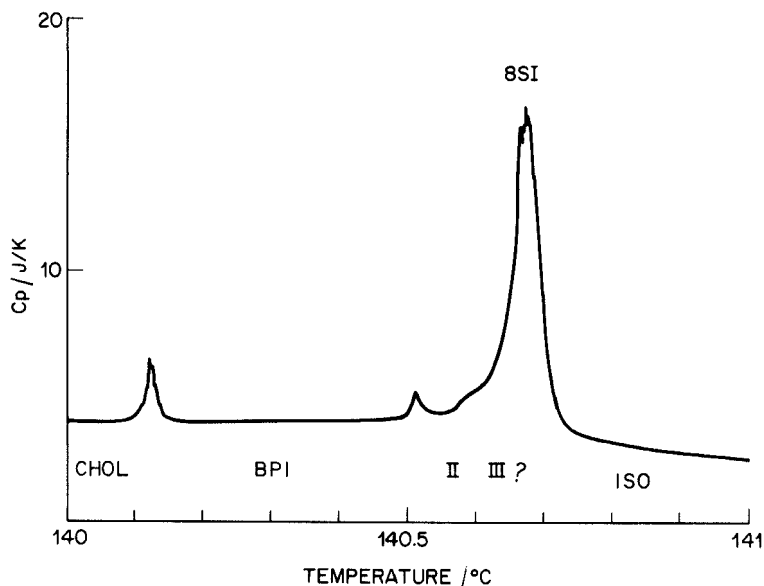


Figure 9. Heat capacity of 8SI\* measured with high resolution, slow scanning calorimetry. Sample mass is 1.38 g. The blue phase transitions are clearly observed. The largest peak is about the same width as observed for CN and CM, materials that are significantly less pure than 8SI\* (compare figures 1, 2 and 3.).

Figure 9 shows the heating run for 8SI\*. The astonishing feature here is that the width of the BPII–isotropic transition is not instrumentally limited in this case even though this sample is believed to be the purest compound studied. It is comparable to CN, a material that is estimated to be significantly less pure. The largest peak is at 140.64°C with a latent heat of 0.1110 cal/g. The BPI–BPII transition occurs at 140.51°C with a latent heat of 0.0023 cal/g and the cholesteric–BPI transition at 140.12°C with 0.0071 cal/g. However, the total heat capacity, 0.1204 cal/g, is smaller by nearly one-fourth of that measured by D.S.C. in this study. The total temperature range of the blue phase region is 0.5°C agreeing with the 0.62°C range observed by optical microscopy.

A small flat peak suggests that there may be a BPII–BPIII transition at about 140.6°C, just before the final transition to the isotropic phase. Only two very bright blue phases are observed by optical microscopy in the visible range. But, we cannot totally exclude the possibility of a BPIII phase that is difficult to observe when its reflections are at very short or very long wavelengths.

### 3. Discussion

#### 3.1. Scan rate and impurity content

The discrepancies in the absolute magnitude for the total latent heats obtained at these much slower scanning rates compared to the D.S.C. results is puzzling. For

transitions of magnitudes 0.5 cal/g, the D.S.C. is not usually off by factors of two and three. The only explanation we have to account for this discrepancy is that perhaps an unusually long time is required for the transition to occur in thermal equilibrium because, for example, the impurity concentration is rather low in these samples so a relatively long time is required for them to migrate to defect cores of the blue phase. Even 0.5°C/min may be too fast a scanning rate for the time constants of blue phase transitions of purer compounds.

Some evidence supporting this notion is that the magnitude of the heats of transition was found to depend on the temperature scanning rate. For example, when CM was scanned at 10°C/min, the cholesteric–isotropic transition occurred at 83.99°C with a latent heat of 0.44 cal/g and yet at a scanning rate of 0.5°C/min, the latent heat was found to be only 0.25 cal/g. Similarly for CN, at 2°C/min, the latent heat is found to be 0.28 cal/g compared to 0.2 cal/g found at 0.5°C/min.

Usually, the magnitude of the heats of transition is independent of scanning rates when thermal equilibrium is maintained in the two D.S.C. chambers. The larger discrepancy for CM suggests that CM requires longer time scales than CN to be in equilibrium through a transition because it has a smaller impurity content. 8SI\* is the purest material we studied and it exhibited the largest discrepancy. If this suggestion is correct, then CN, CM and 8SI\* were out of equilibrium even at the slowest scanning rate of the D.S.C. 0.5°C/min.

But the largest discrepancy is observed for 8SI\*, which we believe to be the isomerically purest of the three compounds. We are forced, therefore, to conclude that the dynamics of segregating the enantiomers, with the least abundant enantiomers migrating to the cores of the defects is more complicated than it is for impurities that are chemically less related to the host material. To quantitatively study these transitions, scanning rates two to three orders of magnitude slower than provided by a standard D.S.C. seem essential.

### 3.2. *The temperature domain of blue phases and impurities*

The surprising result of the high resolution measurements is that no difference is observed in the widths of the heats of transition between an essentially chemically pure compound, such as 8SI\* and one that was substantially less pure, such as the VS stock of CN. Neither the purer nor the less pure material showed instrumentally narrow heat capacity versus temperature curves as expected from thermodynamic considerations. This result leads to the conclusion that the presence of the R enantiomer in 8SI\* contributes to as much of a broadening of this transition as chemically different impurities do in CN, for example.

In hindsight, perhaps this conclusion is not too surprising. Mixtures of left and right handed chiral species in liquid crystals, rarely mix in an ideal fashion. Phase transition temperatures of the racemate are frequently either lower or higher than that of the chiral species. For cholesteric materials exhibiting blue phases, the nematic to isotropic transition temperature of the racemic equivalent is typically lower than the blue phase to isotropic transition temperature. Because it is energetically favourable for the impurity species to exist at interfaces and in the cores of defects, the surface energy is effectively reduced thereby stabilizing large super-molecular structures of double twist that can then be organized into blue phases.

Taking this conclusion together with results on the impurity content of the cholesteryl esters measured at 220 nm, then the total temperature spanned by the blue phases,  $\Delta T_{BP}$ , systematically shrinks nearly linearly with increasing purity (figure 10).

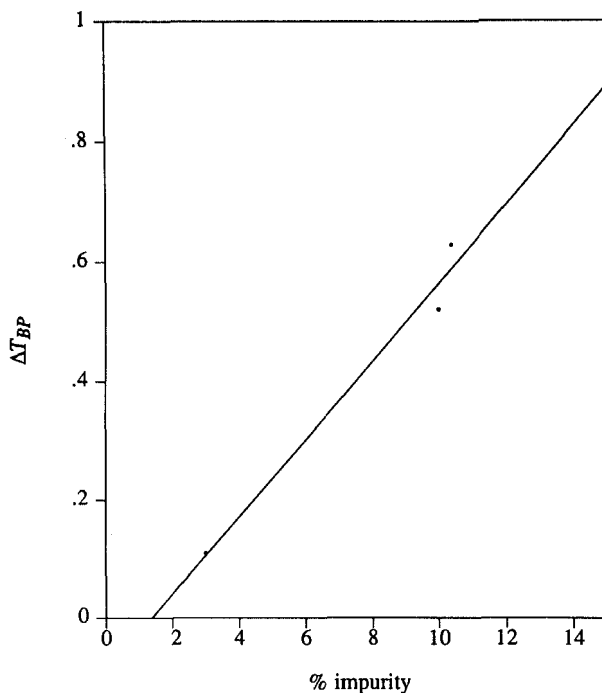


Figure 10. Temperature range of blue phases versus concentration of chiral impurities. From left to right in the figure, the samples are: CM, 8SI\* and CN.

The linear best fit to the three points is

$$\Delta T_{BP} = -0.09 + 0.07x$$

with  $x$  the percentage of impurity. A linear extrapolation of these results suggests that materials with somewhat less than 1.3 per cent impurity, where the opposite handed enantiomer is included in the impurity estimate, would not exhibit blue phases. Because we believe the impurity levels used are a lower limit for the cholesteryl esters, this estimate is also a lower limit.

### 3.3. Materials with two asymmetric centres

Do we know of any cholesteric materials to support this conclusion? Perhaps. A long standing puzzle has been, why don't the tightly twisting compounds, 4M6Cl (S,S-4-[(4'-methylhexyloxy)benzoyloxy]-2-chlorophenyl 4-(4'-methylhexyloxy)-benzoate) and 2M4Cl (S,S-4-[(2'-methylbutyloxy)benzoyloxy]-2-chlorophenyl 4-(2'-methylbutyloxy)benzoate) show blue phases? 8SI\* has one chiral and one non-chiral aliphatic chain. The class of compounds, pMqCl has two chiral aliphatic chains. Although pMqCls exhibit tightly twisted cholesteric phases of pitch in the 0.3  $\mu\text{m}$  to 0.14  $\mu\text{m}$  range, they do not exhibit blue phases. Figure 11 shows the amusing boojum-like objects that appear as the cholesteric phase of 4M6Cl condenses from the isotropic liquid.

One reason these materials do not exhibit blue phases may be related to the fact that these substances are composed of two complimentary pairs of diastereoisomers

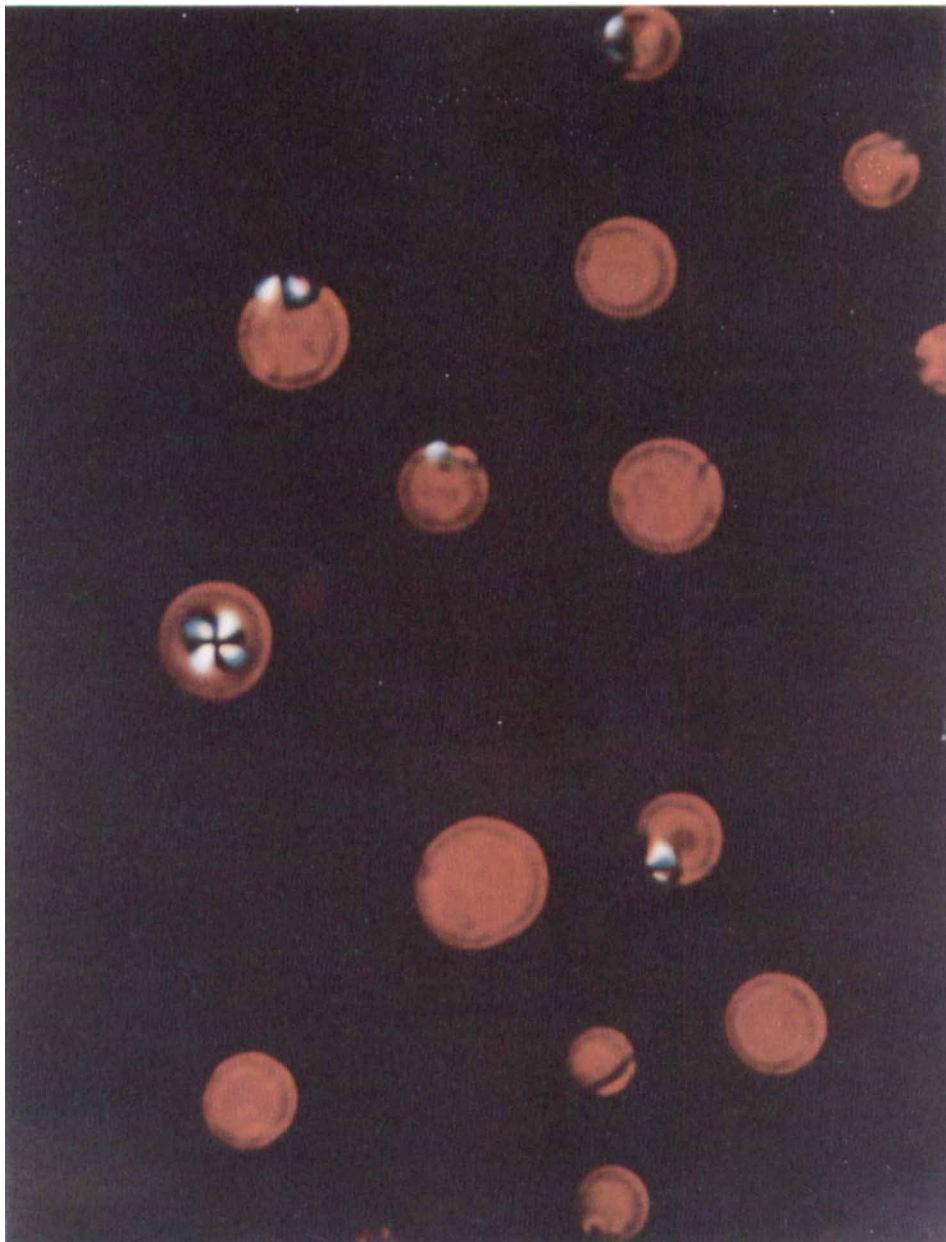


Figure 11. Boojum-like droplets that condense from the isotropic phase when the diastereoisomer (4M6Cl) transforms to the cholesteric phase. Although these materials are tightly twisted, they do not exhibit blue phases. The racemate exhibits similar drops. In the photomicrograph, the droplets are seen to be highly asymmetric. The 'front' of the drop is decorated with a white background with a black cross in the centre. The 'back' of the drop is smooth and red. Profiles of the droplets are also seen.



and enantiomers. The relative purity of the two sets of pairs is a direct function of the relative optical purity of the starting reagent S-2-methylbutanol obtained from Fluka. This substance was found to be a mixture of 90 per cent of the S isomer and 10 per cent of the R isomer. The preparation of materials with two chiral centers obtained from this same starting material results in a mixture of two pairs of enantiomers: the RR–SS and the RS–SR isomers. Each pair of enantiomers are also diastereoisomers of the other pair, for example, the RR material is the diastereoisomer of the SR or the RS compound. Thus, for a ratio of 9:1 of the S to R isomers in the original starting alcohol, the final products will contain mole fractions of 0.01 RR, 0.09 RS, 0.09 SR and 0.81 SS of compounds with two chiral centers. Consequently, for the SS and RR enantiomers, the enantiomeric excess of the SS isomer is 0.988, i.e. the mixture only contains 1.2 per cent of the opposite RR enantiomer. Thus, the optical purity has effectively increased compared to what would be obtained for a mono-chiral centre species, like 8SI\*.

The SR and RS enantiomers in pMqCIs are present in equal amounts and so form a racemic mixture—a nematic—that acts like a neutral isomer. On this basis they would not necessarily appear as impurities to the RR–SS enantiomeric pairs since, as is well-known, nematics tend to mix ideally with cholesterics whereas enantiomers often produce non-ideal behavior.

Tentatively, the relative difference in mixing behavior may be understood on the basis of steric arguments. Half of an RS or SR molecule is identical to its SS and RR isomers encouraging like-packing attributes. In addition, some selected bond rotations could enhance this diastereoisomeric packing even more so that the steric hindrance between RR (or SS) and SR (or RS) is not as severe as between RR and SS isomers. Consequently, diastereoisomeric packing may appear in some substances as more ideal than enantiomeric packing. Therefore, we argue, the minority enantiomer would tend to be localized at the core of defects in the phase, the fraction so segregated being a function of the concentration of the isomer. Thus, at low concentrations, fewer defects can be stabilized energetically than at higher concentrations of impurities.

We emphasize that we are not suggesting this as a separations process for optical isomers. Rather, in dynamical systems, exemplified by liquid crystals in general, we suggest that there will be a somewhat higher fraction of the minority isomer at defect cores raising interesting new possibilities for the microscopic structure of blue phases and ‘boojums’.

#### 4. Conclusions

We have measured the heats of transition and assessed the impurity content of three chiral compounds exhibiting blue phases. Because the heat capacity peak at the blue phase to isotropic liquid transition is not resolution limited, even in 8SI\*, the isomerically purest compound we studied, we were lead to include any enantiomer of the opposite hand to that of the predominant enantiomer as an impurity. This lead to a monotonic dependence between sample purity and the temperature domain of blue phase formation that merits further study on other compounds. We also observed the magnitude of the total latent heats of blue phase transitions to be a sensitive function of scanning rates. To obtain reliable quantitative heat capacity data, we conclude that scan rates two to three orders of magnitude slower than provided by a standard D.S.C. apparatus are essential.

## References

- [1] BELYAKOV, V. A., and DMITRIENKO, V. E., 1985, *Usp. Fiz. Nauk.*, **146**, 369; 1985, *Sov. Phys. Usp.*, **28**, 534.
- [2] CLADIS, P. E., *IMA. Vol. 5. Theory and Applications of Liquid Crystals*, edited by J. L. Ericksen and D. Kinderlehrer (Springer-Verlag), p. 73; SETHNA, J. P., *ibid.*, p. 99.
- [3] SETHNA, J. P., 1985, *Phys. Rev.*, **31**, 6278.
- [4] FINN, P. L., and CLADIS, P. E., 1981, *Molec. Crystals liq. Crystals Lett.*, **72**, 107.
- [5] MEIBOOM, S., SETHNA, J. P., ANDERSON, P. W., and BRINKMAN, W. F., 1981, *Phys. Rev. Lett.*, **46**, 1216; MEIBOOM, S., SAMMON, M., and BRINKMAN, W. F., 1983, *Phys. Rev. A*, **27**, 438.
- [6] GRAY, G. W., and McDONNELL, D. G., 1976, *Molec. Crystals liq. Crystals* **37**, 189.
- [7] GOODBY, J. W., and GRAY, G. W., 1979, *J. Phys., Paris*, **C3-40**, 27.
- [8] STEGEMEYER, H., and BERGMANN, K., 1980, *Liquid Crystals of One and Two-dimensional Order*, edited by W. Helfrich and G. Heppke (Springer-Verlag), p. 174.
- [9] LEON FONG, and BETTY, M., 1982, *IXth International Liquid Crystal Conference*, Bangalore.
- [10] TANIMOTO, K., CROOKER, P. P., and KOCH, G. C., 1984, *Phys. Rev. A*, **32**, 1893.
- [11] ARMITAGE, D., and PRICE, F. P., 1975, *J. Phys., Paris*, **36**, C1-113.
- [12] KLEINMAN, R. N., BISHOP, D. J., PINDAK, R., and TABOREK, P., 1984, *Phys. Rev. Lett.*, **53**, 2137.